

New apparatus for Skid Testing: Assessment for Dusty Surface

Head Researcher: PM Dr Abdul Aziz b Chik

Researcher: Mr Liew Taik Hwa

Funded by: UTM 71937

1.0 Introduction

Traffic accidents have been the nation concern. In year 2000, there are 5.6 fatalities per 10,000 registered vehicles. This figure is amongst the highest in the ASEAN region. Factors contributed to traffic accidents can be categorized into three main categories. These are the human, vehicle and road. However, engineers can only addressed the engineering aspects through proper design procedures and audits. There are many well-developed design procedures either for geometry or structural design of the roadways. It is unfair to say that the high accident rate is because of the poor design. The specification is often more conservative than expected. Thus, apart from the design aspect, the possible answers may be due to the roadway features. Roadway features such as the landscape, debris on the road surface and pavement defects are the reasons that often been ignored. Road surface debris is the most forgotten aspect during maintenances. Debris like oil, fine aggregates, plastic bags, dust on the road surface and even bricks are often left on roadway to be exposed off. Although there are no statistical data on accident that really cause by roadway debris, we cannot exclude the possible effects on road user's safety. It is more significant for motorcycles and light vehicles where they always travel on nearside lanes. Motorcycles share a high proportion of Malaysian traffic. In year 2000, there are 5.4 million registered motorcycles or 50.5% of total vehicles. The needs of cyclist on the roads and segregated from other users have been overlooked, thus it may be one of the reasons for the high fatality. Compare to cars and other heavier vehicles, a motorcycle is much more sensitive to the effect of pavement skid property especially when maneuvering at corners. This study is aim at addressing the above problem in relation to the motorcycles and to develop a fundamental skidding property on a dusty pavement.

1.1 Problem Statement

Skid resistance act as a friction force when a vehicle moves. It is an important property for safe maneuver of vehicles. The effect of dust surface on the road surface is highly significance to motorcycle where its maneuver depends largely on the balance and stability of the friction force. Riding hazard occurs when motorcycle is side by side with a large vehicle. Large vehicle would travel near center of the road thus motorcycle is force to ride along the dusty path. A slight skidding would end up with an injuries accident. Although there is no actual statistical count of such accident or those slight injuries caused by own crash, the risk of hazard is not to be underestimated. The skid resistance property is controlled by both the pavement and tyre of vehicle. The contact surfaces of both become the key to skid property. Thus, it is of highly importance to identify the effect of dust on road surface toward the skidding resistance property.

1.2 Aim and Objective

The aim of this study is to investigate the option to develop a prototype skidding tester which can model the surface property of a dusty pavement. The loading of a motorcycle will be used as this class is of highly susceptible by such condition. To achieve this aim, the study was designed as follows:

- to establish a related function of a conventional test method with a new tester,
- to develop a prototype laboratory fabrication of the new tester and calibration, and
- to estimate the statistical value for the effect of loose particle on skid resistance.

1.3 Importance of the Study

Motorcycles are the vulnerable vehicle class in the traffic stream. It is of the highest proportion in Malaysian traffic. Effort to segregate from other vehicle class has been going on but of at slow pace. They will continue to use the nearside lane which may be exposed to dusty condition. Skidding resistance act as friction force during movement, thus it is of highly importance to study the effect on such condition as the motorcycle depends on the balance and stability of the friction force.

1.4 Scope of Study

The study focuses on the development of skidding mechanism on a dusty surface. A prototype laboratory skidding frame considering such forces mechanism will be fabricated and calibrated. The loading of a motorcycle, which is of the highest percentage in Malaysian traffic, will be considered. This vehicle class is also the highest percentage of vehicle that involved in road accidents.

ABSTRACT

Skidding has been identified as one of the most common factor for road accident. Skid resistance is also related to several road features, which are the skidding properties of the road surface, the presence of water and contaminants. Many apparatus are designed and has been used to determine the value of the skid property of a road surface under dry and wet conditions. The purpose of this research is to design and fabricate a new apparatus for measuring the skid resistance on dusty surfaces. Calibration and verification have been carried out and two correlation charts are plotted. This research is based on downstream application, i.e. calibration and correlation are carried out with specific condition to have a related function of the conventional test method (British Pendulum Tester) with the new tester. From the results, significant drop of skid number are recorded when loose particles are applied to the samples surfaces. This shows that there is a possibility of skid assessment through friction turning mechanism. However, the tester requires further modification to achieve higher consistency.

LIST OF TABLES**LIST OF FIGURES****CHAPTER ONE
INTRODUCTION**

1.0 Introduction	1
1.1 Aim and Objective	2
1.2 Importance of the Study	2
1.3 Scope of Study	3

**CHAPTER TWO
LITERATURE REVIEW**

2.1 Skidding Resistance	4
2.2 Pavement Texture	5
2.3 Factors affecting the Skid Resistance	6
2.4 Skid Resistance Test	8
2.4.1 British Pendulum Tester	9
2.4.2 Accelerated Polishing Test	11
2.4.3 SCRIM – Sideway Force Coefficient Routine Investigation Machine	12
2.4.4 Mu-Meter	14
2.4.5 Grip Tester	15
2.5 Sand Patch: TRRL	16
2.6 Skid Resistance and Accident Risk	17

**CHAPTER THREE
DESIGN CONCEPTS**

3.1 Friction Forces acting on Vehicles	18
3.2 The Basic Idea of the Prototype Tester	19
3.3 The Design Components	20
3.4 Assumption and Limitations	25

**CHAPTER FOUR
CALIBRATION AND VERIFICATION**

4.1 Calibration and Correlation Charts	26
4.2 Effect of Loose Particles	27
4.3 Impact Scale	28
4.4 Texture Depth, Coefficient of Friction and Load Scale	29
4.5 Correlation Chart	32
4.6 Verification	35

**CHAPTER FIVE
APPLICATION, ANALYSIS AND CONCLUSIONS**

5.1 Contaminant Effect	38
5.2 Discussions	39
5.3 Conclusions and Recommendations	40
REFERENCES	41
APPENDIX A – TESTING PROCEDURE OF SFT	42
APPENDIX B - DATA	44

CHAPTER TWO

LITERATURE REVIEW

Understanding of the forces mechanism at skidding is essential to study and develop the prototype laboratory model that can explain the interaction of forces. This Chapter describes the theoretical aspect of the related functions transfer and the major studies associated with skidding phenomena.

2.1 Skidding Resistance

Skid occurs when a vehicle brakes, accelerates, or maneuvers during which the frictional force exceeds the limiting friction force that can be generated at the tyre and road interface (Kennedy et al, 1988). The two principal forces acting on a vehicle tyre at the tyre and road interface are the vertical force (normal load) F_V due to the weight of the vehicle and the horizontal frictional force F_H which is the reaction to the braking force. Thus the frictional force has a limiting value given by:

$$F_H = \mu F_V \quad \text{Equation 2.1}$$

where:

μ is the coefficient of friction between the tyre and the road. When the vehicle is braking in a straight line, there is no lateral forces and,

$$\mu = \frac{\text{braking force}}{\text{vertical force}} \quad \text{Equation 2.2}$$

When wheel is about to skid, the braking force is at its maximum and μ is referred as the peak braking-force coefficient or the coefficient of impending sliding. When the wheel is actually skidding, the braking force is slightly lower, μ in this condition is known as the braking-force coefficient. When a vehicle is turning, the wheels are at an angle relative to the direction of the

motion and a sideways force is induced. Side slip of the tyre will occur when the sideways force exceeds the limiting value and is given by:

$$\mu = \frac{\text{sideway force}}{\text{vertical force}} \quad \text{Equation 2.3}$$

and, in this condition, μ is known as the sideway-force coefficient. Braking-force coefficient and the side-way force coefficient are the two most common measures for skid resistance. Normally, braking-force coefficient is 0.8 times the side-way coefficient (Croney, 1991).

2.2 Pavement Texture

The main properties that govern the skid resistance of a road are their micro and macro texture. Large-scale texture in the range of 0.5 to 15mm (macrotexture) and small-scale texture in the range up to 0.5mm (microtexture) are both important in determining overall skid resistance. Figure 2.1 shows the macrotexture of a pavement surface. The texture depth is the depth between the emerge edge of the aggregates to the binder.

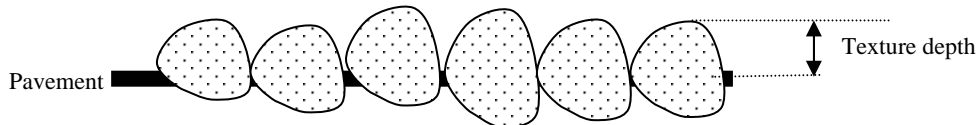


Figure 2.1: Texture Depth

Fine texture of the exposed aggregates is important in the design of non skid flexible surfaces, can be examined microscopically, but for routine purpose, it is generally assessed by measurements of the coefficient of friction determined by a rubber slider moving over a prepared sample of the aggregate set in cement mortar bed (Croney, 1991). Figure 2.2 shows the classification of the surface texture.

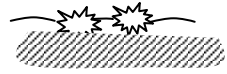
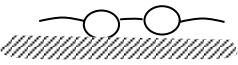
surface		Scale of texture	
		macro	micro
A		rough	harsh
B		rough	polished
C		smooth	harsh
D		smooth	polished

Figure 2.2: Illustration terms used for describing surface texture (Kennedy, et al, 1988)

Both micro and macro texture affect the skid resistance of a pavement. Rough and harsh pavement texture will perform better, while polished and smooth texture will have an adverse effect. Rough surface also has better drainage capability and this can reduce the risk of hydroplaning (build up of thin layer of water, Kennedy, et al, 1988). Normal considerations consider the wet surface (during rains) as the most critical level for skid resistance. Hence, skid resistance testing is carried out with the present of water.

Dry pavements are usually not slippery, but there are a number of things that can make a pavement slippery which sometimes worse than wet surface. Slippery may also develop from surface contamination, such as the oil spillage or certain types of loose particles (TRRL, 1969).

2.3 Factors affecting the Skid Resistance

The factors that influence the skid resistance with an indication of the magnitude of their effect are given in Table 2.1 For tropical countries like Malaysia, where seasonal variation is hardly identified, the influence of wet season is of the most critical factor.

Table 2.1: Factors affecting the Skid Resistance (Asphalt Institute, 1983)

Factor	Type	Typical Variation in SFC (sideway-force coefficient)
Climate	<ul style="list-style-type: none"> Seasonal Variation (wet/dry cycles) Temperature 	<ul style="list-style-type: none"> ± 0.12 $0.003/^{\circ}\text{C}$
Traffic	<ul style="list-style-type: none"> Daily flow of commercial vehicles braking, Acceleration, centrifugal force 	<ul style="list-style-type: none"> 0.06 per 1000 CV per day 0.05
Surfacing	<ul style="list-style-type: none"> Coarse aggregate type (asphalt surfacing) Contamination: Dust, rubber, etc Texture depth (sand patch) <ul style="list-style-type: none"> Asphalt 2.0mm Concrete 0.8mm Asphalt 1.0mm Concrete 0.5mm 	<ul style="list-style-type: none"> 0.01 for each unit reduction in PSV 0.10 No change with speed 20% reduction with speed change from 50 to 130 km/h

Based on the Table above, temperature also affects the skid resistance where the rubber resilience and hysteresis losses become smaller as temperature rises. These effects combine to reduce the measured value of skid resistance as temperature increases. The effect is not particularly significant over the normal working range of temperature, but it can be significant when the equipment with non-continuous types of operation is used. Increasing temperature reduces SFC by 0.003 units per $^{\circ}\text{C}$ (Table 2.2) but, surfacing with high coefficient of friction tends to suffer a greater reduction (Salt, 1977). A major factor, which determined the skid resistance of a bituminous surface containing a high proportion of aggregate at the tyre/road interface is the polishing resistance of the aggregate (PSV). As shown in Table 2.1, every unit change in PSV corresponds to about 0.01 changes in mean sideways-force coefficient for the same traffic intensity (Hosking and Woodford, 1976). Both the compressive strength of the aggregate affects the skid resistance of a concrete road. However, the characteristics of the coarse aggregate have little effect (Franklin and Calder, 1974). Skid resistance of the surface of both flexible and concrete roads also varies immensely with the commercial traffic density. A relatively lower skid resistance value is at sites where horizontal forces are set up (braking, acceleration or failing to maintain the correct speed/superelevation relationship on bends). Sideways-force coefficient can be expected to be 0.05 or lower at this type of locations (Hosking and Tubey, 1973).

2.4 Skid Resistance Tests

Skidding (loss of adhesion between a vehicle tyres and the road surface) occurs in many road accidents whether or not it is the actual cause of the accidents. Over the years, tyre manufacturers have conducted research into different types of rubber and tread patterns to improve the safety of motor vehicles. Highway engineers have also explored into the material properties and construction methods to improve the skidding resistance of road surfaces.

The first invented device is the Pendulum Skid Tester, being portable, can be taken to the site or being used in the laboratory. Pendulum Skid Tester simulates the skid resistance by a road surface to a car traveling at 50 km/h. The result gives a number, being a percentage, which is the coefficient of friction for the surface tested against standard rubber. Subsequently, the Sideways Force Coefficient Routine Investigation Machine (SCRIM) was developed. This is a lorry with a fifth wheel set at an angle to the direction of travel and the lateral force on this wheel is measured and recorded. The lorry travels at 50 km/h and continually monitors the sideways-force coefficient (SFC). Other devices include, braking force trailer and the mu-meter for the same purpose and can be used at high speed especially for airport runways.

When considering the material used in the construction of pavement, highway engineers are concerned about the aggregates. Transport Road Research Laboratory (TRRL) also devised the Accelerated Polishing machine, which simulates the polishing action of tyres, grits and water on road surfaces. The aggregates undergo six hours of polishing actions and then tested with the pendulum for the polished stone values (PSV).

The equipments mentioned above can be classified into two major types:

Pendulum Skid Tester and Accelerated Polishing Machine are for laboratory used, while SCRIM, Mu-Meter, the Pendulum Skid Tester and Braking Force Trailers are for in-situ purposes.

2.4.1 British Pendulum Skid Tester

Procedure for the used of the Pendulum Skid Tester is published by TRRL,1969 and is shown in Table 2.2.

Table 2.2: Procedure for the application of pendulum skid tester (Yoder and Witczak, 1975)

step	Description
1	Select the spot/sample under study
2	Apparatus is then sets (Figure 2.3) on the sample/road so that the slider will swing in the direction of traffic flow and level the base screws.
3	Raise the swinging arm clear of the sample/road and clamp in the horizontal position. Release the arm and check that the pointer reads zero.
4	With the pendulum arm free and hanging vertically, place the spacer, attached to a chain on the base of the column, under the lifting handle setting screw to raise the slider. Lower the head of the tester so that the slider just touches the sample/road surface and clamp in position. Remove the spacer.
5	The sliding length of the rubber slider over the sample/road surface is checked by gently lowering the pendulum arm until the slider just touches the surface first on one side of the vertical and then on the other. When passing the arm through the vertical, use the lifting handle so that the slider does not touch the road. The sliding length should be between 125 and 127 mm. If not, adjust by raising or lowering the head.
6	Place the pendulum arm in the horizontal and clamp in position.
7	Wet the sample/road surface and slider with water.
8	Bring the pointer to its stop then release the pendulum by pressing the button. Take care to catch the arm on its return swing before it hits the ground.
9	Return the arm and pointer to the release position keeping the slider off the sample/road surface by means of the lifting handle. Repeat the test, wetting the surface between swings. Record the mean of five successive readings, provided they do not differ by more than three units. If the range is greater than this, repeat swings until three successive readings are constant; record this value.
10	Record the temperature of the water on the sample/road surface.

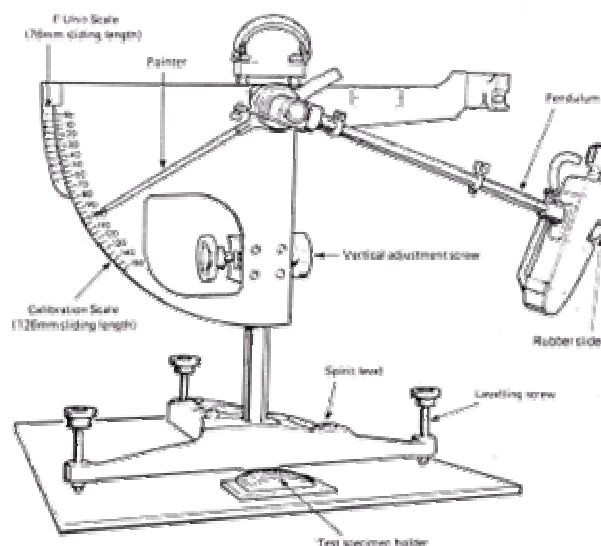


Figure 2.3: Pendulum Skid Tester (BSI, 1990)

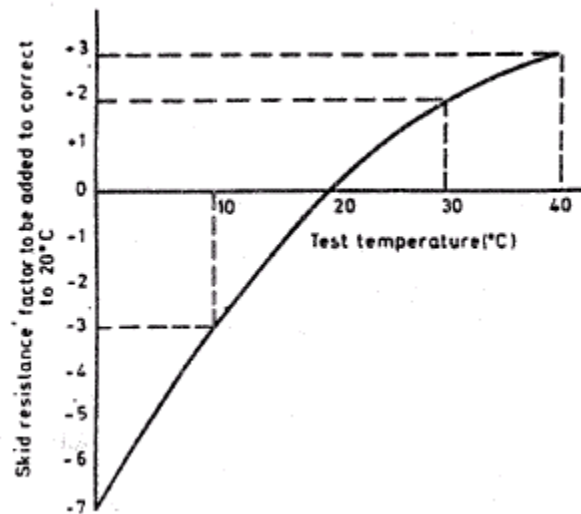


Figure 2.4: Skid resistance/ temperature correction relationship (TRRL 1969)

As the stiffness of the rubber slider will vary with temperature, a correction has to be made if the temperature is not 20°C by using the temperature curve (Figure 2.4).

However, the tester is not suitable for the used on surfaces covered with mud or fine particles. The slider tends to sweep away the mud or fine particles (Giles, et al, 1964). Because of the plough action, surface covered with loose particles is virtually impractical to be tested by the pendulum tester. Table 2.3 shows the minimum PSV (sample/surface) suggested for different types of road by Portable Skid Tester (PST).

Table 2.3: Suggested minimum values of Skid Resistance for PST (Yoder and Witzak, 1975)

Category	Type of Sites	Min skid resistance (wet surface)
A	Difficult sites such as: <ul style="list-style-type: none"> • Roundabouts • Bends with radius less than 150m on unrestricted roads • Gradients 1 in 20 or steeper of lengths greater than 100m • Approaches to traffic lights on unrestricted roads 	65
B	Motorways, trunk and class 1 roads and heavily trafficked roads in urban areas (carrying more than 2000 veh per day)	55
C	All other sites	45

2.4.2 Accelerated Polishing Test

The purpose of this test is to give a relative measure of the degree of polishing of aggregates under traffic condition (Shahin, 1994). The test consist of two separate steps, the first is the accelerated polishing machine and secondly by the pendulum skid tester. Figure 2.5 shows the accelerated polishing machine.

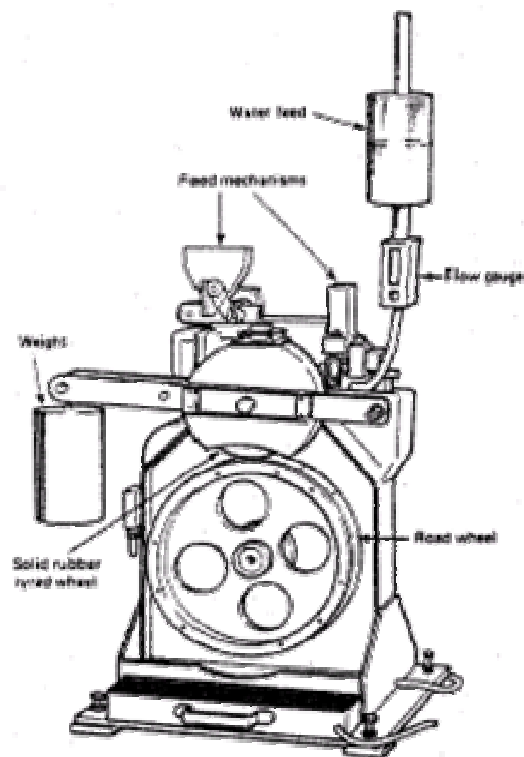


Figure 2.5: Accelerated Polishing Machines (BSI, 1990)

The accelerated polishing machine has a road wheel with a flat periphery (45mm wide and 406 mm in diameter) and of such a size and shape that 14 specimens can be clamped around the periphery so as to form a continuous surface of aggregate particles. The wheel rotated about its axis at a speed of 315 to 325 rev/min (Shahin, 1994). The first 3 hours, water and corn emery grits are fed continuously onto the surface of the specimens. The machine and the specimen are washed thoroughly and then continue for another 3 hours but fed with water and air-floated emery

flour. The specimen are then removed from the machine and tested using the portable skid resistance tester.

Table 2.4: Minimum Polished Stone Coefficients for Bituminous Roads (Hosking, 1992)

Site	Definition	Commercial Vehicles (CV) per lane/day	Min PSV
A1 (very difficult)	<ul style="list-style-type: none"> Approaches to traffic signals on road with speed limit greater than 64 km/h Approaches to traffic signals, pedestrian crossings and similar hazards on main urban roads 	Less than 250 CV/lane/day	60
		250 to 1000 CV/lane/day	70
		1000 to 1750 CV/lane/day	70
		More than 1750 CV/lane/day	75
A2 (difficult)	<ul style="list-style-type: none"> Approaches to major junctions on roads carrying more than 250 commercial vehicles per lane per day Roundabouts and their approaches Bends with radius less than 150m on roads with speed limit greater than 64 km/h Gradients of 5% or steeper, longer than 100m 	Less than 1750 CV/lane/day	60
		1750 to 2500 CV/lane/day	70
		2500 to 3250 CV/lane/day	70
		More than 3250 CV/lane/day	75
B (average)	Generally straight sections of and large radius curve on: <ul style="list-style-type: none"> Motorways Trunk and principal Other roads carrying more than 250 commercial vehicles per lane per day 	Less than 1750 CV/lane/day	55
		1750 to 4000 CV/lane/day	60
		More than 4000 CV/lane/day	65
C (easy)	<ul style="list-style-type: none"> Generally straight sections of lightly trafficked roads Other roads where wet accidents are unlikely to be a problem 	-	45

The mean value as determined is reported as the PSV. The minimum polished stone coefficients for bituminous roads depending on their functions are shown in Table 2.4.

2.4.3 SCRIM – Sideway Force Coefficient Routine Investigation Machine

SCRIM was designed by TRRL and is used to measure the wet skidding resistance of a road surface (Kennedy, et al, 1988). The measurements of skidding resistance recorded are used to identify the length of a road that are below investigate levels defined for a range of different site categories. It is ideal for network skidding resistance surveys and has daily survey capacity of 200

to 300 km depending upon road type. Figure 2.6 and 2.7 shows the SCRIM model. The vehicle normally operates at 50 km/h for testing, but on certain model, the measurement can be made at speed up to 80 km/h.



Figure 2.6: SCRIM – Sideway Force Coefficient Routine Investigation Machine

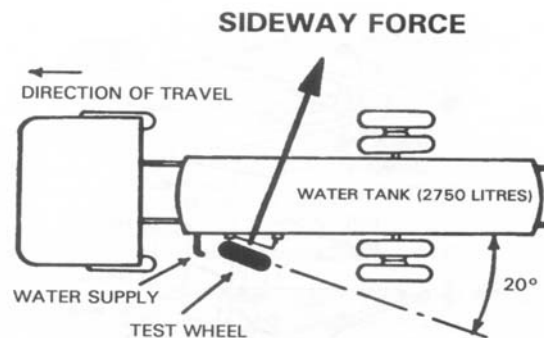


Figure 2.7: Plan View of SCRIM

Test wheel mounted at mid-vehicle, in both the nearside and offside wheel paths at an angle of 20 degrees to the direction of travel. The test wheel, which has a smooth pneumatic tyre of standard hardness, is freely rotating and is applied to the road under a constant vertical load of 200 kg. A controlled flow of water wets the road surface immediately in front of the test wheel. When the vehicle moves forward, the test wheel slides in forward direction on a wet road surface. The force generated by the resistance to skidding is related to the wet skidding resistance of the wet road surface.

2.4.4 Mu-Meter

The Mu-Meter is a side-force measuring trailer, with two of the three wheels on the trailer unit are positioned at 7.5° from the center axis of the trailer. This produces an apparent slip ratio of 13.5° while the third wheel is for distance measurement. The schematic diagram is shown in Figure 2.8. Computer equipment records and produces a strip chart with continuous friction values versus distance traveled.

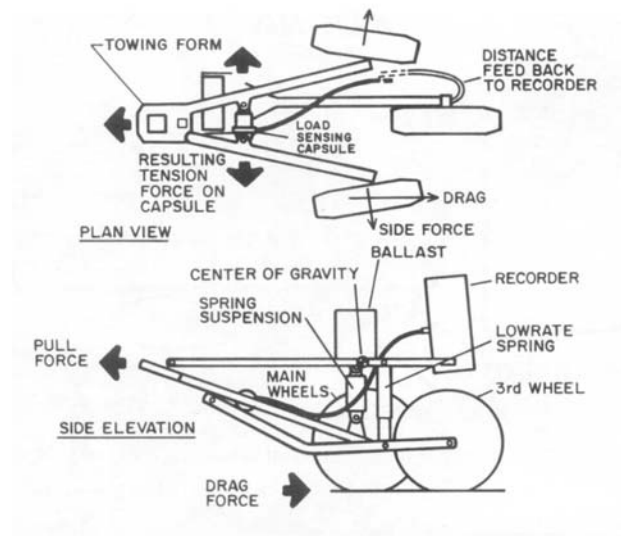


Figure 2.8: Schematic diagram of Mu-Meter



Figure 2.9: Mu-Meter Attached to A Jeep

This is actually similar the SCRIM, however Mu-Meter is more flexible for its small size attachment as shown in Figure 2.9. Recent application had improved the Mu-Meter with self-wetting system.

2.4.5 Grip Tester

Figure 2.10 shows the arrangement of a Grip Tester, which is the most versatile friction tester available. It is used at large and small airports all over the world both for the maintenance and operational testing.



Figure 2.10: Grip Tester

Grip tester is a three wheel machine that is towed by a suitable vehicle with approximately 1 meter long and 60cm wide (Technical Committee, 1987). Water is supplied to the test wheel as all skid resistance value relate to the wet road surface. The two driving wheels are on single axle, the driving force from this axle is connected to the test wheel but is geared down so that the test wheel must rotate more slowly than the driving wheel, thus creating a braking force on the test wheel. When the wheel rolls freely, its slip ratio is 0%, but when it is locked, its slip ratio is 100%. The Grip Tester has a measuring wheel slip ratio of just over 15% which is suitable for airport and highways. The friction coefficient (load/drag) is known as Grip Number, is transmitted to a data collection computer.

2.5 Sand Patch: TRRL

This procedure was developed by TRRL and was one of the first methods used to calculate surface texture (Hosking and Woodford, 1976). This involves spreading of a known volume of fine, dry sand over a circular area until flush with aggregates tips of the pavement surface (Figure 2.11).

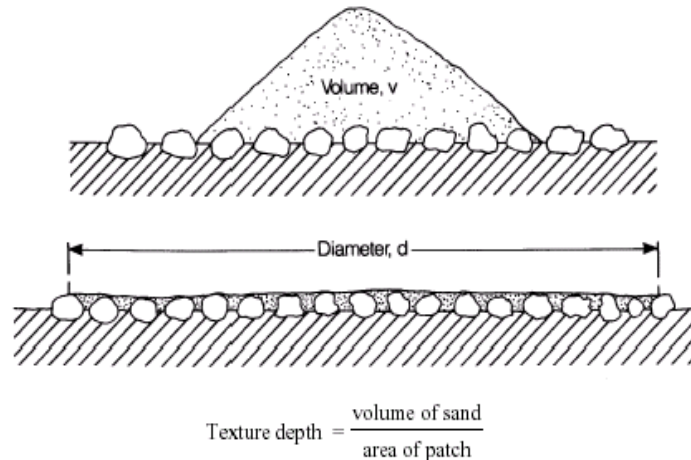


Figure 2.11: Sand-patch method of measuring texture depth

The area of this patch is determined from an average of several diameter measured and the texture depth can be calculated by dividing the known sand volume to the patch area.

There are other equipment used to assess the skidding property and the texture of a pavement. From a survey carried out by the Land Transport Safety of New Zealand, test methods used by 29 authorities for assessing the skidding property are SCRIM 35%, British Pendulum Tester 29%, Grip Tester 16% and Mu-Meter 3%. However, it appears that not much consideration have been made to assess the effect of fine loose particles on the pavement under dry condition. Skid property would be critical during the wet day with the present of thin film of water but, sand and dust would be detrimental in dry condition. It is necessary to provide a possible assessment on a dry dusty surface.

2.6 Skid Resistance and Accident Risk

A relationship between tyre/road surface coefficients and the relative likelihood of repeated skidding were highlighted by Giles (in Salter, 1979). Giles found out that the likelihood increased exponentially as the sideways-force coefficient measured at 50 km/h decreased. For a surface with the coefficient at 0.6 or above the risk of wet weather skidding accidents was extremely small. The risk became measurable with a coefficient between 0.55 and 0.6 and increased rapidly by more than 20 times at a value of 0.4 to 0.45 and by 300 times when the coefficient is 0.3 to 0.35. The newer proposal modified the proposal by Giles adding the super class of high-skid site (Salter, 1979). The minimum values suggested for maintenance program are the site classification and the accidents record. The minimum value of sideways friction coefficient for any given class will depend on the risk rating which also determine by the accident potential sites. From this study, a direct relationship between sideways friction coefficient, traffic flow and polished stone value for bituminous surfaces, whilst another relationship for the skid resistance value , polished stone value, concrete strength and aggregate abrasion value. From the literature search, the risk of accident increases exponentially as skid resistance decreases.

CHAPTER THREE

DESIGN CONCEPTS

The preceding Chapters provide related studies on the skidding resistance evaluation equipment. All of the equipments measured the skidding resistance on a wet surface, which have shown to increase the risk of accidents exponentially. No equipment that is able to estimate the skidding resistance on a contaminated surface. The focus of this study is to measure the change of friction force (tyre/road surface) due to the loose particles trapped between the contact areas of the tyre/road surface. This Chapter describes the basic idea and the design concepts of the prototype model of the surface friction skid tester (SFT).

3.1 Friction Forces acting on Vehicles

The ratio of forces, the frictional coefficient μ is governed by two major aspects, which is the frictional properties of the contact surfaces and the effective contact area of both surfaces. In order to make a stable maneuver, the total forces acting on the vehicle should equal to zero or positive friction force/centrifugal force ratio. Superelevation is often introduced to maintain the positive ratio. Figure 3.1 shows the forces acting on the vehicle on curves.

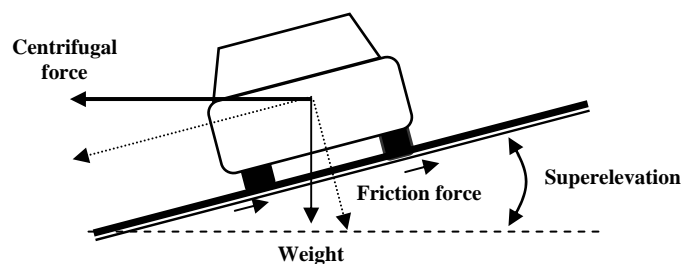


Figure 3.1: Forces on Vehicle at Curve

Centrifugal force is governed by three variables, these are the turning radius, speed and superelevation. Friction forces exist as two surfaces grip each other. Thus its depends on the frictional characteristics of both the grip surfaces. High frictional property would provide a better grip between surfaces. However, this may change if there exist loose particles in between the

surfaces. Figure 3.2 shows the likely effect of loose particles between the surfaces. The presence of dust will reduce the contact surface.

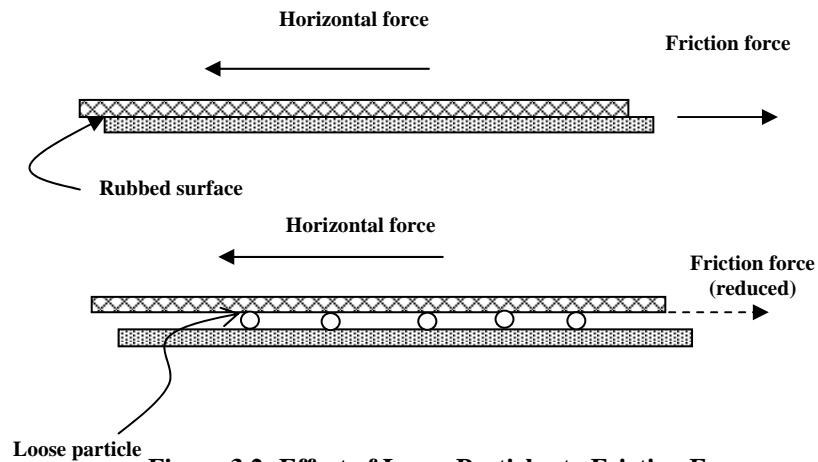


Figure 3.2: Effect of Loose Particles to Friction Force

3.2 The Basic Idea of the Prototype Tester

From the review of the existing apparatus for skid resistance, there are no suitable apparatus that can be used to assess the contaminated surface. Hence, the prototype model is developed to imitate the skidding action of a tyre/road surface with the loose particles trap between the contact surfaces. When an impact is applied, the surface will rub against each other and the friction effect can be measured. The basic idea of the set up is shown in Figure 3.3.

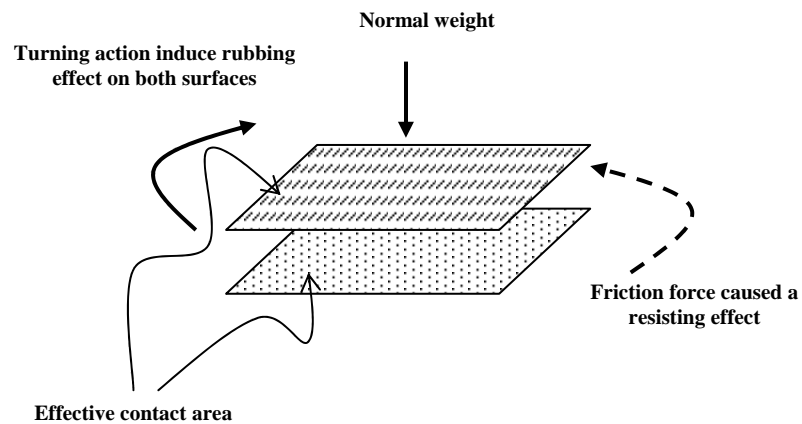


Figure 3.3: Basic Idea of Friction Forces of the Model

As British Pendulum Skid Tester (BPT) and the design concept of the prototype model have similar turning mechanism, a comparison can be made with BPT skid number to obtain a direct transfer function.

3.3 The Design Components

The functions shown in Figure 3.3 are transformed for the design of Surface Friction Tester (SFT). If the arrangement is as in Figure 3.4, the tester is able to accommodate the presence of loose particles on the contact surfaces. The design principle of the SFT provides certain variable control of the testing condition, which is the normal load, impact magnitude and contaminants type. A test plate is used with the conventional standard rubber used for the pendulum tester. This will reduce the possible variation between the new tester and the BPT during the calibration.

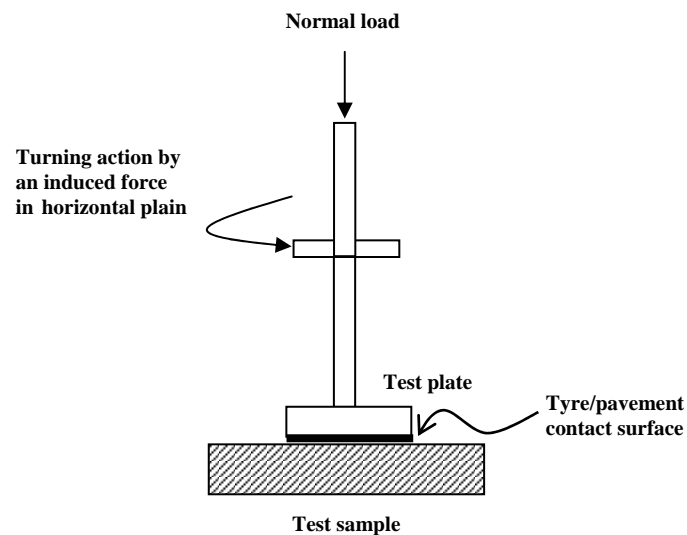


Figure 3.4: Working Principle for SFT Model

As the plate is rectangle, pressure on the test sample can be calculated directly from the applied load. The pressure can be changed to suit the required condition. The load pressed the rubber against the sample as the test is run. The mechanism of the rubbing action is shown in Figure 3.5.

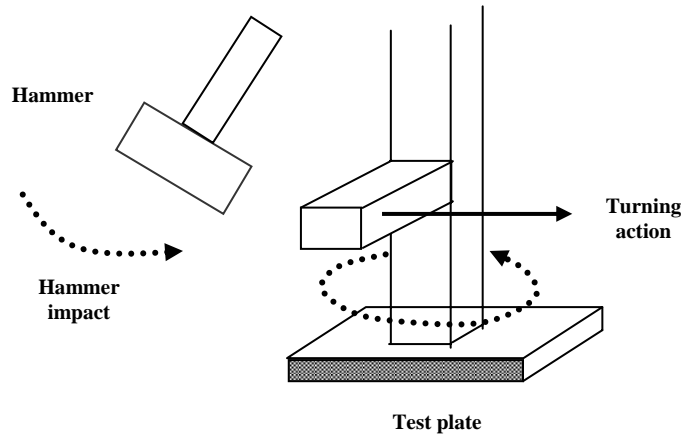


Figure 3.5: Rubbing Action on Hammer Impact

Based from Figure 3.5, the hammer impact is calculated by dynamic equation for pendulum. When the hammer is raised, energy is preserved and then the turned into kinetic energy when released. Thus the impact of the pendulum hammer can be determined.

$$U = mgh \quad \text{Equation 3.1}$$

Where:

- U = preserved energy,
- m = mass of object,
- g = gravitational acceleration, and
- h = height of object against datum.

$$K = \frac{1}{2}mv^2 \quad \text{Equation 3.2}$$

Where:

- K = kinetic energy,
- V = object speed,

$$U = K \text{ (conservation energy)}$$

$$\therefore mgh = \frac{1}{2}mv^2$$

$$2mgh = mv^2$$

$$v = \sqrt{2gh} \quad \text{Equation 3.3}$$

since,

$$a_t = \frac{dv}{dt}$$

a_t = tangent acceleration of the pendulum,

$$a_t = \frac{dv}{d\theta} \times \frac{d\theta}{dt}$$

$$= \frac{dv}{d\theta} \times \omega$$

$$= \frac{(v_2 - v_1)}{(\theta_2 - \theta_1)} \times \omega, \quad = \frac{(v_{\max} - 0)}{(\theta - 0)} \times \omega, \quad = \frac{v_{\max}}{\theta} \omega$$

and,

$$\omega = \frac{v}{r}$$

r = radius to center of oscillation,

$$a_t = \frac{v^2}{r\theta}$$

Equation 3.4

By substituting Equation 3.3 into Equation 3.4,

$$a_t = \frac{2gh}{r\theta}$$

Equation 3.5

where:

a_t = tangent acceleration,

g = gravitational force,

h = height of object against datum,

r = length of object to center of oscillation, and

θ = angle of pendulum drop in radian.

Hence:

$$F_t = ma_t$$

$$= \frac{2mgh}{r\theta}$$

$$= \frac{2mgh}{l}$$

Equation 3.6

where:

F_t = impact force, and

l = distance travel by pendulum.

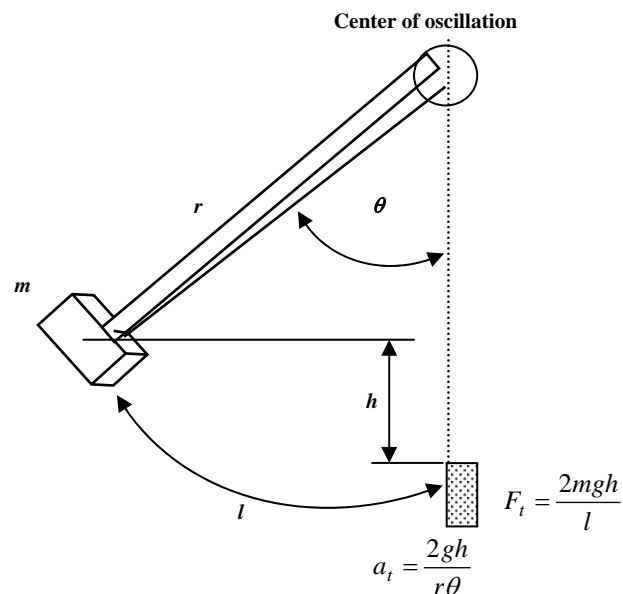


Figure 3.6: Derivation of Forces of Pendulum Impact

Based on the derivation of forces, SFT is fabricated using mild steel to suit the research purposes. The main body unit is able to withstand a maximum stress of 150 kg. The details fabricated parts are as shown in Table 3.1. Photograph in Figure 3.7 shows the developed surface friction skid tester (SFT) that was based on the explained forces derivation.

Table 3.1: Fabricated parts of the Equipment

No	Parts	Quantity	Description
1	Load screw	1	To apply load on the test plate hence creating a load pressure on the rubber/sample surface. The load applied depend on the magnitude required
2	Load transfer bar	1	To transfer the load to the test plate stem. Round edge will help to diminish possible friction between the load screw and the test plate component.
3	Test plate unit	1	Act as the component in the rubbing mechanism in which load is applied through the test plate stem to the plate.
4	Sample plate	1	To hold the test sample during the test.
5	Cross clamp	1 pair	To hold the test plate unit in position during impact.
6	Hammer set	1	To create an impact that will produce the rubbing mechanism
7	Body set	1	The main structure of the equipment

Figure 3.7: The Developed Surface Friction Skid Tester (SFT)

3.4 Assumptions and Limitations

There are several assumptions that were made due to the limitation of the laboratory facilities. In future, these assumptions should be revised and to improve the equipment. The assumptions are summarized as follows:

- Since the calibration of this apparatus is based on a comparison with Pendulum Skid Tester, the result measurements are applicable to vehicle speed of 50 km/h or lower though it tends to give the friction coefficient value for the sample surface itself.
- The effect of normal load from the wheel is insignificant and therefore it is not applied during the initial measure (no friction). As normal load is unlikely to affect the result of initial measure under a zero friction condition.
- Since test sample is not to be used for excessive number of test, the wear effect from both the Pendulum Skid Tester and SFT is considered insignificant. Hence the friction coefficient of the material is constant.
- Friction between the members of the apparatus is small hence insignificant.
- Since the purpose is to measure the friction coefficient of sample surface, element like normal load, temperature and tyre property are not considered.

CHAPTER FOUR

CALIBRATION AND VERIFICATION

The main task of this project is to calibrate and verify the new equipment so as it can act as a load transfer from the British Pendulum Tester. Once a certain degree of confidence has been achieved during calibration and verification, it can be used to study the effect of loose particles between the contact surfaces. This Chapter explained the process of calibration and verification, hence to obtain the calibration charts.

4.1 Calibration and Correlation Charts

A British Pendulum Tester (BPT) is required during the calibration process where the coefficient of friction for the test samples is to be predetermined. Prior to the used, the BPT equipment is calibrated according to ASTM E303 V4.03 manual.

Several tests samples are prepared in a size of 150 x 150 x 75 mm (Asphaltic Concrete Wearing 14) following the size required by the sample plate. Several wear samples are also collected from the existing pavement and cut into size. The sample list is shown in Table 4.1.

Table 4.1: Sample type and label for calibration and verification

SAMPLES	
Type	Label
New Mix Sample (ACW 14)	SA1
	SA2
	SA3
Wear sample from existing pavement (ACW 14)	SB1
	SB2
	SB3
	SB4
	SB5
Independent Wear Sample – reserved for verification (ACW 14)	SC1

Average texture depth is determined using the Sand Patch Method. Coefficient of friction of all samples was predetermined using the BPT. Data for the turning angle due to the specific applied condition are collected and compared with the coefficient of friction fro each sample.

4.2 Effect of Loose Particle

The effect of loose particles on surface skid resistance will be the secondary target of this research. If the direct transfer function is available, the coefficient of friction of the dusty surface can be assessed. There are two options for the loose particles experiment:

- first, by using the percentage of area covered by loose particles,
- second, by using the percentage of texture depth filled with loose particles.

The second option is selected for experiment because it is easier to be determined.

The texture depth of each samples are predetermined using the Sand Patch Method. In order to specify the percentage of filled, the area to be tested is confined using the following:

$$V = A \times d \quad 4.1$$

Where:

V = volume of loose particles,

A = patching area, and

d = estimated texture depth.

The coefficient of friction on dusty surface is calculated using the calibrated correlation charts.

The effect of loose particles on frictional property can then be acquired.

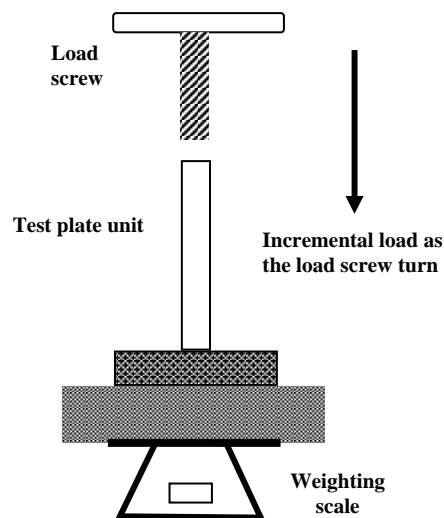


Figure 4.1: Arrangement for Load Scale Test

4.3 Impact Scale

From the energy/impact relationship, there are two variables to be determined in order to obtain the impact force used to turn the plate test unit. Based on Equation 3.6,

$$F_t = \frac{2mgh}{l}$$

where:

F_t = impact force, and

l = distance travel by pendulum (m).

Since:

$$r' = \frac{r}{\cos \theta},$$

$$a = r' - r,$$

$$= \frac{r}{\cos \theta} - r \quad 4.2$$

and,

$$h = a \sin \alpha,$$

$$= a \sin (90^\circ - \theta),$$

$$= a \cos \theta \quad 4.3$$

By substituting Equation 4.2 into Equation 4.3:

$$h = r - r \cos \theta \quad 4.4$$

where:

r = hammer arm length (m), and

θ = angle clockwise from vertical axis ($^\circ$).

A series of drop angle value, hammer height and drop impact can be derived from Equation 4.4. The hammer weight is fabricated at 2.89 kg and Table 4.2 shows the deriving value for different drop angle. In order to acquire proper turning movement of the test plate unit, the applied normal load should be less than the impact force.

Table 4.2: Impact Values for Different Angles

Drop angle, θ ($^{\circ}$)	Hammer Height, h (m)	Impact, F_i (N)
10	0.008	4.9
20	0.031	9.8
30	0.068	14.5
40	0.119	19.0
45	0.149	21.1
50	0.182	23.2
60	0.255	27.1
70	0.336	30.5
80	0.421	33.5
90	0.510	36.1

4.4 Texture Depth, Coefficient of Friction and Load Scale

The Sand Patch Method determines texture depth of each sample. Table 4.3 shows the value collected for each sample from the sand patch test. Based on the sample surface area, the texture depth is calculated.

Table 4.3: Volume obtained on Sample Surface and Texture Depth

Sample		Volume (ml)					Texture Depth (mm)
Type	Label	1	2	3	4	Average	
New Sample	SA1	16.5	15.0	15.5	15.0	15.5	0.69
	SA2	17.0	15.0	14.0	15.0	15.3	0.68
	SA3	15.5	15.0	15.0	14.0	14.9	0.66
	SA4	13.0	13.0	14.0	13.0	13.3	0.59
Wear Sample	SB1	38.0	41.0	41.0	41.0	40.3	1.82
	SB2	31.5	29.0	30.5	29.0	30.0	1.33
	SB3	42.0	42.0	43.0	41.0	42.0	1.87
	SB4	38.0	36.0	35.0	38.0	36.8	1.66
	SB5	41.0	43.0	43.0	42.5	42.4	1.90
Reserve Sample	SC1	30.5	31.5	31.0	31.0	31.0	1.38

Skid resistance test on the sample is carried out using the British Pendulum Tester (BPT). Based on the skid resistance number from the BPT, Equation 4.5 below is used to determine the coefficient of friction. Each of the skid number is adjusted for a room temperature of 28 °C using the skid resistance/temperature correction chart.

$$\text{Skid Resistance} = \frac{300 \rho \mu}{3 + \mu} \quad 4.5$$

Table 4.4 shows the calculated Coefficient of Friction from the BPT skid resistance number.

Table 4.4: Coefficient of Friction of Each Sample

Sample		Dry Surface		Wet Surface	
Type	Label	BPT Skid Number	Coefficient of Friction, μ	BPT Skid Number	Coefficient of Friction, μ
New Sample	SA1	100	1.304	72	0.837
	SA2	102	1.342	79	0.944
	SA3	100	1.304	76	0.898
	SA4	96	1.231	74	0.867
Wear Sample	SB1	97	1.249	63	0.708
	SB2	93	1.177	59	0.653
	SB3	92	1.160	64	0.722
	SB4	86	1.057	57	0.626
	SB5	107	1.439	78	0.929
Reserve Sample	SC1	97	1.249	78	0.929

The first calibrating element of the surface friction tester (SFT) is its load scale. Since the normal load is applied by lowering the load screw, and angle scale (1°) is attached to the load screw where the relationship of incremental load turning degree can be calibrated. Several sets of data with specific angle increment were collected and the average increment loading is as shown in Table 4.5. A load scale equation is also derived from the relationship as in Equation 4.6.

Table 4.5: Load Scale

Angle (°)	Load (g)	Angle (°)	Load (g)
0	0	70	2077
5	108	75	2200
10	276	80	2280
15	432	85	2380
20	595	90	2502
25	746	95	2606
30	919	100	2741
35	1077	105	2887
40	1235	110	3043
45	1388	115	3234
50	1515	120	3434
55	1662	125	3641
60	1810	130	3770
65	1941		

The value in Table 4.5 is based the average of 12 load tests, whilst Equation 4.6 below is obtained from the linear regression of the data. The R^2 value is 0.9957. The turning angle is taken as zero when the test plate first touches the scale.

$$L = 28.6\delta \quad 4.6$$

Where:

L = load (g), and

δ = turning angle (°).

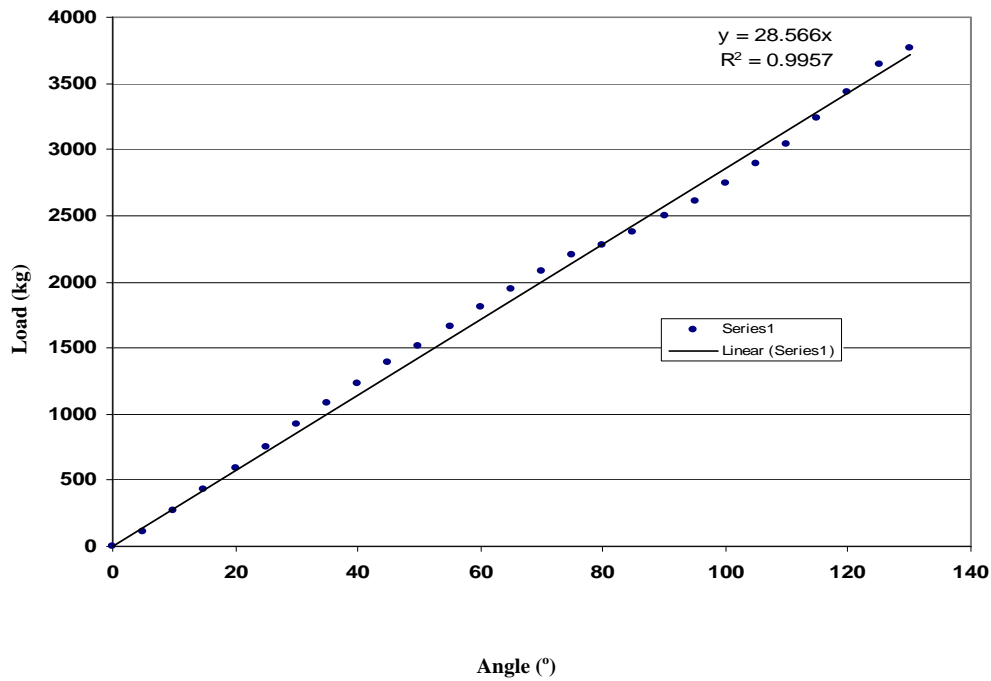


Figure 4.2: Load and Turning Movement Relationship

4.5 Correlation Chart

A set of data containing 25 observations on interval of 5° is collected to calculate the average turning angle of each test. Two sets of tests with different loading are observed. First, with a normal load of 1.3 kg with an interval of 5o hammer drop (30° to 50°). The second, with a normal load of 1.785 kg with an interval of 5° hammer drop (35° to 55°). Both are subjected to the dry and wet condition. The minimum induced forced for the second test is increased because of the additional normal load where a higher force is required to make the minimum turning readable by the apparatus. The average value for each interval is shown in Tables 4.6a and 4.6b. Exponential plots are used to correlate the relationship and the correlated function. Table 4.7a and Table 4.7b show the correlated function of skid number and turning angle with its subsequent R^2 value. Subsequently, two correlated charts with different normal load and surface condition between the turning angle, d and skid number SN are plotted. These are shown in Figures 4.3 and 4.4.

Table 4.6 a: Average Turning Angle for Different Drop Angle ~ Normal Load 12.75N

sample	SN:BPT	Hammer Drop Angle, 'θ', Normal Load=12.75N: Dry				
		30	35	40	45	50
SA1	100	35	47	58	65	77
SA2	102	23	30	37	48	57
SA3	100	36	43	50	58	66
SA4	96	48	58	64	71	80
SB1	97	45	62	77	90	99
SB2	93	41	63	74	84	96
SB3	92	48	63	78	84	99
SB4	86	52	69	82	90	101
SB5	107	38	55	70	84	89
SC1	97	40	52	62	69	81

Table 4.6 b: Average Turning Angle for Different Drop Angle ~ Normal Load 17.51N

sample	SN:BPT	Hammer Drop Angle, 'θ', Normal Load=17.51N: Dry				
		35	40	45	50	55
SA1	100	24	32	41	51	62
SA2	102	22	31	38	48	61
SA3	100	24	31	41	49	56
SA4	96	32	43	50	59	66
SB1	97	31	42	59	72	83
SB2	93	35	46	61	76	88
SB3	92	36	51	64	75	91
SB4	86	44	56	70	79	94
SB5	107	27	40	54	66	75
SC1	97	30	39	51	63	72

Table 4.7a: Transfer Function ~ Normal Load = 12.75N

Normal Load: 12.75N: Dry		
Hammer Drop Angle, 'θ'	Relationship	R ²
30	$\frac{100}{d} = 0.1679e^{0.0282SN}$	0.9241
35	$\frac{100}{d} = 0.0789e^{0.0331SN}$	0.8980
40	$\frac{100}{d} = 0.0665e^{0.033SN}$	0.8501
45	$\frac{100}{d} = 0.0801e^{0.0298SN}$	0.8618
50	$\frac{100}{d} = 0.0829e^{0.028SN}$	0.7873

Table 4.7b: Transfer Function ~ Normal Load = 17.51N

Normal Load: 17.51N: Dry		
Hammer Drop Angle, 'θ'	Relationship	R ²
35	$\frac{100}{d} = 0.025e^{0.0511SN}$	0.9980
40	$\frac{100}{d} = 0.0166e^{0.0522SN}$	0.9695
45	$\frac{100}{d} = 0.0108e^{0.0541SN}$	0.9970
50	$\frac{100}{d} = 0.0122e^{0.0507SN}$	0.9751
55	$\frac{100}{d} = 0.014e^{0.0475SN}$	0.9175

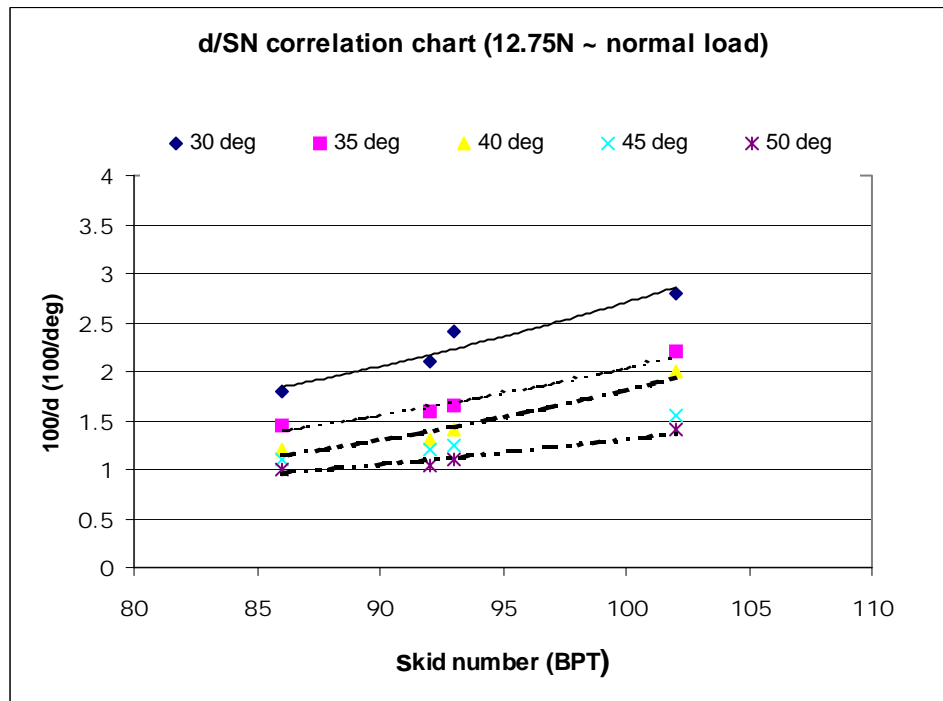


Figure 4.3: Correlation Chart normal load 12.75 N

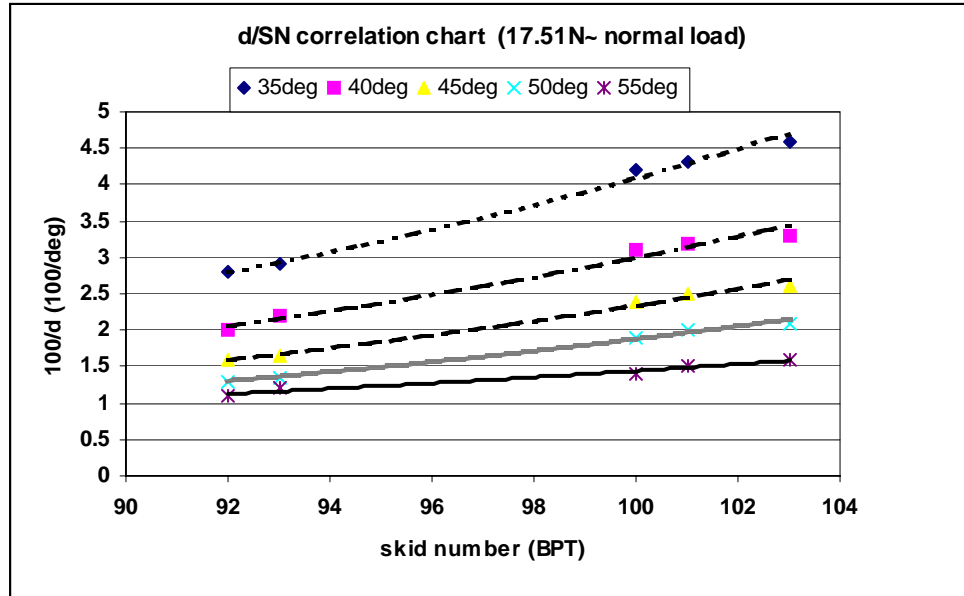


Figure 4.4: Correlation Chart normal load 12.75 N

4.6 Verification

The correlation charts shown in Figure 4.3 and Figure 4.4 are then verified using the reserved samples (SC1). The observations also consist of 25 tests on each interval (5°). The measured values are quite closed to the predicted plot values with slightly higher deviation for lower normal load and minimum induced force. Figure 4.5 and 4.6 shows that the results provide an average deviation of 1.2 for Correlation Chart A and 1.8 for Correlation Chart B. Another set of data is taken using the normal load of 12.75N and a sphere globe instead of test sample. The sphere globe provides a minimum contact area between the surfaces to determine the consistency of induced force applied. The result shows smooth distribution of exponential plot as shown in Figure 4.7 with a high value of R^2 . This result has a similar trend as those individual tests during the calibration where almost all showed smooth exponential distribution.

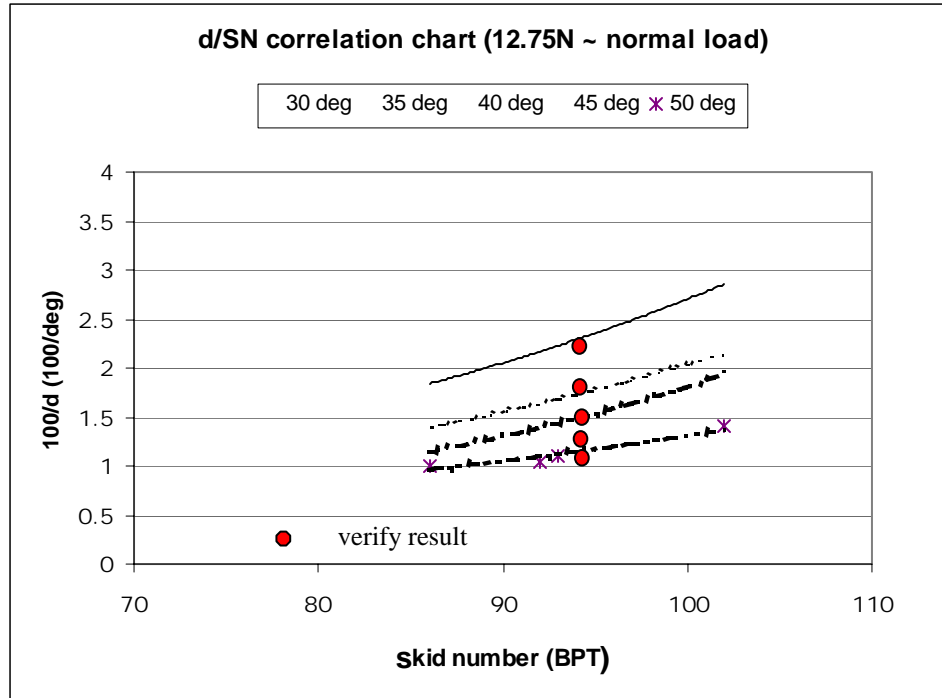


Figure 4.5: Correlation chart A (verification result -12.75N normal load)

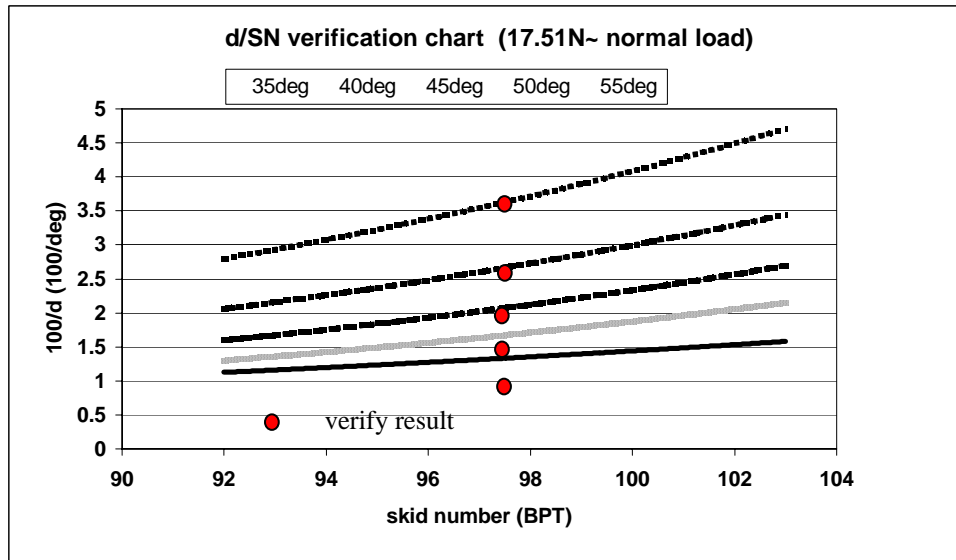


Figure 4.6: Correlation chart B (verification result -17.51N normal load)

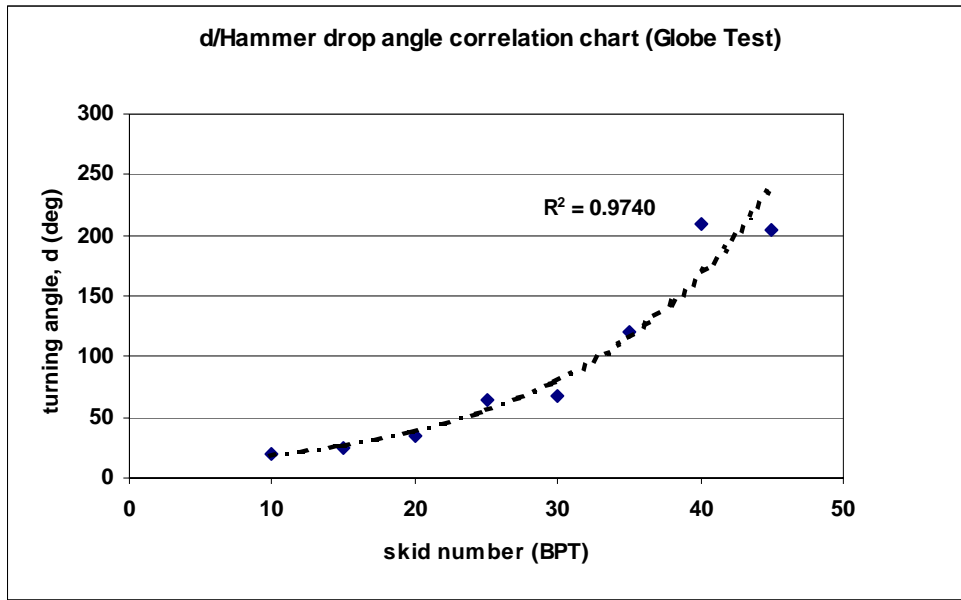


Figure 4.7: Globe Test drop angle

CHAPTER FIVE

APPLICATION, ANALYSIS AND CONCLUSIONS

Chapter 4 has described the process of calibration, verification and validation of the skid resistance model. This Chapter discusses the application, analysis and interpretations to obtain the value of skid resistance of the contaminants surfaces. The original data can be obtained from the Appendices.

5.1 Contaminant Effect

Three selected samples are tested in the same way as the calibration and validation process. Two levels of loose particles are used (full texture depth, excessive thickness 2-3 mm). A set of data consist of 25 tests run on each interval of 5° are collected to acquire the average turning angle for each test condition. The test conditions are used are the same with those used during the calibration process. The details of each test are as summarized in Table 5.1. A total of 317 samples are prepared for rigorous testing to ascertain the skid number for the contaminant effects. Some samples are cored and trimmed using the masonry cutter to fit into the moulds. The varying number of samples indicates the shortage of sampling characteristics for the chosen parameters.

Table 5.1: Application test details

No	No of samples	Type of texture	Particle size	Load (N)
1	50	Full texture depth	75 μ m	12.75
2	44	Excessive thickness	75 μ m	12.75
3	25	Full texture depth	75 μ m	17.51
4	40	Excessive thickness	75 μ m	17.51
5	50	Full texture depth	150 μ m	12.75
6	43	Excessive thickness	150 μ m	12.75
7	25	Full texture depth	150 μ m	17.51
8	40	Excessive thickness	150 μ m	17.51

There are significant drop of the skid number when the loose particles are spread over the sample surface. Full texture depth filled with dust particles does not show strong effect of friction loss. However, excessive thickness of loose particles does show greater effect towards skid number.

The skid test and the results are shown in Table 5.2. The result shows not much different between different types of particles. The results are similar to those suggested by Kennedy et al (1988).

Table 5.2: Estimated Skid Number for Dusty Surface

Sample	Original Surface SN	Dusty surface			
		Particle size 75µm		Particle size: 150µm	
		Full texture depth	Excessive thickness	Full texture depth	Excessive thickness
SA1	100	95	95	87	86
SB3	92	87	86	80	80
SC1	97	91	92	83	84

5.2 Discussions

There are several notable errors in the calibration process that may have altered the consistency of the correlation charts which is shown by the lower R^2 values (coefficient of determination). One from the British Pendulum Tester and the other from the developed mechanism. These two are the likely reasons for the errors. Also the minimal error which could be the parallax during reading, thus the position of the vision when taking the data should be adjusted to suit the operator.

It is also important to have a perpendicular aligned sample where the sample is perfectly settled in the sample plate. Slight displacement can effect the turning movement of the test plate unit. This problem is encountered during some of the observations. However, there may be also some possibility that this may occur unnoticed. A mechanism such as the bubble spirit level is of helpful for adjustment purposes.

The accuracy of the correlation charts can be improved, however, at this stage it does provide guidance for further calibration processes. Problems also exist in the form of the lack of standard for comparison. Based on the results, it can be concluded that the trends is similar compared to the available source of reference. Better correlation can be obtained if there were more reliable references for comparison.

Further study and modification of the developed Skid friction Tester is necessary if a more reliable and consistent tests and results are to be obtained. The tester fabricated to measure the

contaminant road surface is considered operational and viable for future modification. The mechanism and the derived forces are suitable for used.

5.3 Conclusions and Recommendations

When considering the risk of accident cause by contaminants, it actually increased the risk of accident with merely a slight drop of 0.1 of coefficient of friction. In order to promote safer roadway for road users, a more systematic road-keeping program should be enforced. Salt and Szatkowski (in Salter, 1979) stressed that the maintenance program should include the road classification and the accident records. The Works Ministry does introduce a prevention monitoring system in Malaysia through the Road Safety Audit in order to identify the problem locations or stretches. However, it still overlooked the uncontrolled debris and surface dust particularly those carried by falling trucks or overflow of water.

A comprehensive monitoring suggests frequent contaminated locations should be identified and warned. Industrial vehicles plying on the public roads should be checked. This experimental study and assessment shows, the skid property of a contaminated road can be measured and analysed. Compared to the conventional tester, this developed skid friction tester uses simpler forces mechanism concept. The equipment is simple and basically based on the rubbing actions of two surfaces.

APPENDIX A

TESTING PROCEDURE OF SFT

This procedure contains three parts

Normal load:

1. Normal load applied to the sample comes from the test plate unit (1.3kg), load transfer shaft (0.485kg), and load screw (over 1.785kg)
2. User can select the normal load accordingly with the help of load scale relationship (normal load kg \sim 28.6 x turning angle of load screw °)
3. No additional load is required if Correlation Chart (test plate unit) or B (test plate unit + load transfer shaft).

Preparation of Sample:

1. The sample used for testing should have a minimum size of 100mm x 100mm and not more than 160mm x 160mm. Round sample (coring sample) can be used with proper modification to the sample plate. Samples of different thickness can be used but not more than 75mm.
2. the sample is then place into the sample plate with sand bedding and leveled using spirit level. The sample is locked into place after it is leveled.
3. Proper combination of test plate unit and load transfer shaft is inserted into the center tube of main body unit. The test plate should be pushed upward to allow the placement of sample plate.
4. The sample plate with the sample inside it (or added with contaminant) is then placed into position at the center of the main body unit, beneath the test plate unit.
5. The cross bar is then fixed to the test plate unit and the column of main body unit. This is to avoid possible lateral movement during the test.
6. Additional normal load can be applied through the load screw if required.

Taking Readings:

1. The datum angle of the test plate unit should be determined. The datum is determined by placing the test plate unit in such a way that its extended side bar touches the pendulum hammer at rest. The datum is recorded and the test plate unit will be reset to this datum after each observation.
2. Raise the pendulum hammer to the required angle and release it. The test plate unit will turn and the reading is recorded. The actual turning angle is acquired by subtracting the final reading with the datum.
3. 15 to 25 consecutive observations are recommended and the average number is used to determine its equivalent skid number.

APPENDIX B

DATA

Normal Load: 12.75 N (average)											
sample	SN	Dry surface					Wet surface				
		Turning angle, d					Turning angle, d				
		30	35	40	45	50	30	35	40	45	50
SA1	100	35	47	58	65	77	36	45	53	62	70
SA2	102	23	30	37	48	57	24	28	36	46	59
SA3	100	36	43	50	58	66	40	47	56	63	70
SA4	96	48	58	64	72	80	52	62	68	75	86
SB1	97	45	62	77	90	99	51	71	88	103	113
SB2	93	41	63	74	84	96	50	70	76	88	107
SB3	92	48	63	78	84	99	50	67	81	93	107
SB4	86	52	69	82	90	101	58	69	85	96	107
SB5	107	38	55	70	84	89	47	74	73	85	103
SC1	97	40	52	62	69	81	50	63	66	75	88

Normal Load: 17.51N (average)											
sample	SN	Dry surface					Wet surface				
		Turning angle, d					Turning angle, d				
		35	40	45	50	55	35	40	45	50	55
SA1	100	24	32	41	41	62	30	39	49	64	74
SA2	102	22	31	38	38	61	27	38	42	51	68
SA3	100	24	31	41	41	56	30	35	44	56	62
SA4	96	32	43	50	50	66	38	50	61	68	74
SB1	97	31	42	59	59	80	38	54	71	80	95
SB2	93	35	46	59	61	88	42	52	71	82	96
SB3	92	36	51	61	64	90	50	60	78	87	105
SB4	86	44	56	64	70	94	56	70	80	90	106
SB5	107	27	40	54	54	75	35	53	62	77	84
SC1	97	35	40	45	45	55	30	39	49	64	74

Normal Load: 12.75 N: loose Particles 75 μm (average)											
sample	SN	Full Texture Depth					Excessive Depth				
		Turning angle, d					Turning angle, d				
		35	40	45	50	55	35	40	45	50	55
SA1	100	41	54	64	76	84	51	69	84	96	104
SA2	102	N/A	N/A	N/A	N/A	N/A	N/A	N/A	N/A	N/A	N/A
SA3	100	N/A	N/A	N/A	N/A	N/A	N/A	N/A	N/A	N/A	N/A
SA4	96	N/A	N/A	N/A	N/A	N/A	N/A	N/A	N/A	N/A	N/A
SB1	97	N/A	N/A	N/A	N/A	N/A	N/A	N/A	N/A	N/A	N/A
SB2	93	N/A	N/A	N/A	N/A	N/A	N/A	N/A	N/A	N/A	N/A
SB3	92	52	69	84	98	110	69	89	97	112	126
SB4	86	N/A	N/A	N/A	N/A	N/A	N/A	N/A	N/A	N/A	N/A
SB5	107	N/A	N/A	N/A	N/A	N/A	N/A	N/A	N/A	N/A	N/A
SC1	97	41	63	75	89	99	59	84	96	106	120

Normal Load: 17.51N loose Particles 75 μm (average)											
sample	SN	Full Texture Depth					Excessive Depth				
		Turning angle, d					Turning angle, d				
		35	40	45	50	55	35	40	45	50	55
SA1	100	29	38	47	56	66	41	53	66	79	104
SA2	102	N/A	N/A	N/A	N/A	N/A	N/A	N/A	N/A	N/A	N/A
SA3	100	N/A	N/A	N/A	N/A	N/A	N/A	N/A	N/A	N/A	N/A
SA4	96	N/A	N/A	N/A	N/A	N/A	N/A	N/A	N/A	N/A	N/A
SB1	97	N/A	N/A	N/A	N/A	N/A	N/A	N/A	N/A	N/A	N/A
SB2	93	N/A	N/A	N/A	N/A	N/A	N/A	N/A	N/A	N/A	N/A
SB3	92	42	54	67	84	95	66	85	105	118	131
SB4	86	N/A	N/A	N/A	N/A	N/A	N/A	N/A	N/A	N/A	N/A
SB5	107	N/A	N/A	N/A	N/A	N/A	N/A	N/A	N/A	N/A	N/A
SC1	97	31	41	57	69	80	51	71	83	92	112

Normal Load: 12.75N loose Particles 150 μm (average)											
sample	SN	Full Texture Depth					Excessive Depth				
		Turning angle, d					Turning angle, d				
		35	40	45	50	55	35	40	45	50	55
SA1	100	41	55	61	78	86	58	68	86	96	106
SA2	102	N/A	N/A	N/A	N/A	N/A	N/A	N/A	N/A	N/A	N/A
SA3	100	N/A	N/A	N/A	N/A	N/A	N/A	N/A	N/A	N/A	N/A
SA4	96	N/A	N/A	N/A	N/A	N/A	N/A	N/A	N/A	N/A	N/A
SB1	97	N/A	N/A	N/A	N/A	N/A	N/A	N/A	N/A	N/A	N/A
SB2	93	N/A	N/A	N/A	N/A	N/A	N/A	N/A	N/A	N/A	N/A
SB3	92	53	69	85	98	110	68	89	96	113	129
SB4	86	N/A	N/A	N/A	N/A	N/A	N/A	N/A	N/A	N/A	N/A
SB5	107	N/A	N/A	N/A	N/A	N/A	N/A	N/A	N/A	N/A	N/A
SC1	97	40	61	76	85	94	59	78	89	106	115

Normal Load: 17.51N loose Particles 150 μm (average)											
sample	SN	Full Texture Depth					Excessive Depth				
		Turning angle, d					Turning angle, d				
		35	40	45	50	55	35	40	45	50	55
SA1	100	30	37	47	56	67	40	52	66	78	103
SA2	102	N/A	N/A	N/A	N/A	N/A	N/A	N/A	N/A	N/A	N/A
SA3	100	N/A	N/A	N/A	N/A	N/A	N/A	N/A	N/A	N/A	N/A
SA4	96	N/A	N/A	N/A	N/A	N/A	N/A	N/A	N/A	N/A	N/A
SB1	97	N/A	N/A	N/A	N/A	N/A	N/A	N/A	N/A	N/A	N/A
SB2	93	N/A	N/A	N/A	N/A	N/A	N/A	N/A	N/A	N/A	N/A
SB3	92	41	55	67	84	96	67	84	103	116	133
SB4	86	N/A	N/A	N/A	N/A	N/A	N/A	N/A	N/A	N/A	N/A
SB5	107	N/A	N/A	N/A	N/A	N/A	N/A	N/A	N/A	N/A	N/A
SC1	97	31	32	56	69	80	51	71	84	93	111

Normal Load: 12.75 N											
sample	Hammer angle	Dry Surface Test					Wet Surface Test				
	30	40	39	40	38	37	31	37	35	36	36
		38	34	35	37	32	35	36	35	36	36
		37	38	34	35	33	34	32	37	38	35
		32	36	32	36	34	31	36	34	37	34
		32	35	34	34	37	37	34	35	36	36
	Average	35					36				
	35	40	39	40	38	37	31	37	35	36	36
		38	34	35	37	32	35	36	35	36	36
		37	38	34	35	33	34	32	37	38	35
		32	36	32	36	34	31	36	34	37	34
32		35	34	34	37	37	34	35	36	36	
Average	35					36					
40	40	39	40	38	37	31	37	35	36	36	
	38	34	35	37	32	35	36	35	36	36	
	37	38	34	35	33	34	32	37	38	35	
	32	36	32	36	34	31	36	34	37	34	
	32	35	34	34	37	37	34	35	36	36	
	Average	35					36				
45	45	40	39	40	38	37	31	37	35	36	36
		38	34	35	37	32	35	36	35	36	36
		37	38	34	35	33	34	32	37	38	35
		32	36	32	36	34	31	36	34	37	34
		32	35	34	34	37	37	34	35	36	36
	Average	35					36				
	50	40	39	40	38	37	31	37	35	36	36
		38	34	35	37	32	35	36	35	36	36
		37	38	34	35	33	34	32	37	38	35
		32	36	32	36	34	31	36	34	37	34
32		35	34	34	37	37	34	35	36	36	
Average	35					36					
SA2	30	40	39	40	38	37	31	37	35	36	36
		38	34	35	37	32	35	36	35	36	36
		37	38	34	35	33	34	32	37	38	35
		32	36	32	36	34	31	36	34	37	34
		32	35	34	34	37	37	34	35	36	36
	Average	35					36				
	35	40	39	40	38	37	31	37	35	36	36
		38	34	35	37	32	35	36	35	36	36
		37	38	34	35	33	34	32	37	38	35
		32	36	32	36	34	31	36	34	37	34
32		35	34	34	37	37	34	35	36	36	
Average	35					36					